

Candidate chiral doublet bands in the odd-odd nucleus  $^{126}\text{Cs}$ Shouyu Wang,<sup>1</sup> Yunzuo Liu,<sup>1,2</sup> T. Komatsubara,<sup>3</sup> Yingjun Ma,<sup>1</sup> and Yuhu Zhang<sup>2</sup><sup>1</sup>Department of Physics, Jilin University, Changchun 130021, People's Republic of China<sup>2</sup>Institute of Modern Physics, Chinese Academy of Sciences, Lanzhou 730000, People's Republic of China<sup>3</sup>Institute of Physics, Tandem Accelerator Center, University of Tsukuba, Ibaraki 305, Japan

(Received 28 November 2005; published 7 July 2006)

The candidate chiral doublet bands recently observed in  $^{126}\text{Cs}$  have been extended to higher spins, several new linking transitions between the two partner members of the chiral doublet bands are observed, and  $\gamma$ -intensities related to the chiral doublet bands are presented by analyzing the  $\gamma$ - $\gamma$  coincidence data collected earlier at the NORDBALL through the  $^{116}\text{Cd}(^{14}\text{N}, 4n)^{126}\text{Cs}$  reaction at a beam energy of 65 MeV. The intraband  $B(M1)/B(E2)$  and interband  $B(M1)_{\text{in}}/B(M1)_{\text{out}}$  ratios and the energy staggering parameter,  $S(I)$ , have been deduced for these doublet bands. The results are found to be consistent with the chiral interpretation for the two structures. Furthermore, the observation of chiral doublet bands in  $^{126}\text{Cs}$  together with those in  $^{124}\text{Cs}$ ,  $^{128}\text{Cs}$ ,  $^{130}\text{Cs}$ , and  $^{132}\text{Cs}$  also indicates that the chiral conditions do not change rapidly with decreasing neutron number in these odd-odd Cesium isotopes.

DOI: [10.1103/PhysRevC.74.017302](https://doi.org/10.1103/PhysRevC.74.017302)

PACS number(s): 27.60.+j, 21.60.-n, 23.20.Lv, 21.10.Re

Chiral doublet bands have been predicted [1] to appear in odd-odd nuclei with substantial triaxial deformation and with configuration where valence proton lies in the lower part of the  $\pi h_{11/2}$  subshell and valence neutron lies in the higher part of the  $\nu h_{11/2}$  subshell in the  $A \sim 130$  mass region. Extensive experimental studies have been made to search for such bands and, as results, candidate chiral doublet bands have been reported in several  $N = 73$  [2],  $N = 75$  [3], and  $N = 77$  [4,5] isotones.

Even-even nuclei with  $A \sim 130$  are known to be  $\gamma$ -soft and under the influences of prolate driving, particle-like,  $h_{11/2}$  proton orbital and oblate driving, hole-like,  $h_{11/2}$  neutron orbital, the odd-odd nuclei with  $A \sim 130$  are expected to have relatively stable triaxial shapes. For odd-odd Cs isotopes with  $A \sim 130$ , the proton Fermi level lies in the bottom of the  $\pi h_{11/2}$  subshell and the neutron Fermi level approaches the top of the  $\nu h_{11/2}$  subshell with increasing neutron number  $N$ . Odd-odd Cs isotopes with larger  $N$  are more suitable for sustaining the chiral geometry than those with smaller  $N$  and thus odd-odd Cs isotopes with larger  $N$  are better candidates for the observation of chiral doublet bands unless the value of  $N$  is too close to  $N = 82$  where the rotational structures are not to be developed. Chiral doublet bands have been reported in  $^{128}\text{Cs}$  [6],  $^{130}\text{Cs}$  [7], and  $^{132}\text{Cs}$  [4]. On the other hand, two positive-parity bands had previously been reported in  $^{124}\text{Cs}$  [8], but in this case they were not interpreted in terms of the chiral rotation. Recently, the data of the two positive-parity bands in  $^{124}\text{Cs}$ , reported in Ref. [8], were systematically compared to those of the chiral doublet bands in  $^{128}\text{Cs}$  and  $^{130}\text{Cs}$  by Koike *et al.* [6] and it was found that the degree of degeneracy and the intraband  $B(M1)/B(E2)$  and interband  $B(M1)_{\text{in}}/B(M1)_{\text{out}}$  ratios of the two positive-parity bands in  $^{124}\text{Cs}$  are similar to those of the chiral doublet bands in  $^{128,130}\text{Cs}$  [6]. This report presents the extended level scheme and  $\gamma$ -intensities of the candidate chiral doublet bands in  $^{126}\text{Cs}$ , and completes the systematic comparison of the electromagnetic properties of the candidate chiral doublet bands in the series of odd-odd Cs isotopes from  $N = 69$  to  $N = 77$ .

Attempting to search for the chiral doublet bands in  $^{126}\text{Cs}$ , high-spin states of  $^{126}\text{Cs}$  were investigated by Li *et al.* [9] and candidate chiral doublet bands in  $^{126}\text{Cs}$  were proposed. However, due to poorer counting statistics, electromagnetic properties of the candidate chiral doublet bands were not discussed in Ref. [9]. The high-spin states of  $^{126}\text{Cs}$  had previously been studied by Komatsubara *et al.* [10] where the coincidence measurements were performed at the NORDBALL, but  $\gamma$ -intensities were not provided in Ref. [10]. It is expected that the counting statistics of  $\gamma$ - $\gamma$  coincidence measurements in Ref. [10] could be much better than that of Ref. [9]. In order to study electromagnetic properties of the chiral doublet bands in  $^{126}\text{Cs}$ , we reanalyzed the  $\gamma$ - $\gamma$  coincidence data collected earlier at NORDBALL by Komatsubara *et al.* [10]. In the present reanalysis of the experimental data collected in Ref. [10], the coincidence data were sorted into a 4096 by 4096 channel symmetrized  $E_\gamma$ - $E_\gamma$  matrix. To obtain information on the  $\gamma$ -ray multipolarities, two asymmetric matrices were constructed and then ADO ratios ( $\gamma$ -ray angular distribution from oriented nuclei) were evaluated using the method as described in Ref. [11]. Typical ADO ratios observed for the known  $\gamma$ -rays were 1.4 for stretched quadrupole or  $\Delta I = 0$  dipole radiations and 0.7 for stretched dipole ones. This empirical law can thus be used to assist us in the multipolarity assignments for newly observed  $\gamma$ -rays. This data set had been utilized previously to establish the high spin structure of  $^{123}\text{I}$  [12]. The detailed experimental setup and procedure were described in Ref. [12].  $\gamma$ -rays assigned to  $^{126}\text{Cs}$  are listed in Table I, together with their  $\gamma$ -intensities, ADO ratios, and spin-parity assignments.

Partial level scheme for  $^{126}\text{Cs}$  derived from the present work is shown in Fig. 1, where band 1 is the yrast band and band 2 is the side band, and the bandhead spin  $I_0 = 9$  of the yrast band was adopted from Ref. [13]. The previously reported positive-parity doublet bands have been extended, for the side band, the odd-spin decay sequence has been extended from  $21^+$  to  $23^+$  and even-spin decay sequence from  $16^+$  to  $22^+$ , and linking transitions 315.5, 739.0, 785.0,

TABLE I. Energies,  $\gamma$ -rays and ADO ratios of  $\gamma$ -rays in  $^{126}\text{Cs}$ .

$E_\gamma$ (keV)	$I_\gamma$ (%)	ADO ratio	$I_i^\pi \rightarrow I_f^\pi$
<b>Band 1</b>			
140.8	100.0(3.0)	0.93(0.06)	(10 <sup>+</sup> ) $\rightarrow$ (9 <sup>+</sup> )
254.8	63.0(6.5)	0.70(0.08)	(12 <sup>+</sup> ) $\rightarrow$ (11 <sup>+</sup> )
337.5	62.2(3.8)	0.65(0.09)	(11 <sup>+</sup> ) $\rightarrow$ (10 <sup>+</sup> )
343.2	17.8(2.6)	0.74(0.11)	(14 <sup>+</sup> ) $\rightarrow$ (13 <sup>+</sup> )
395.7	47.9(3.2)	0.66(0.08)	(13 <sup>+</sup> ) $\rightarrow$ (12 <sup>+</sup> )
415.5	2.5(0.4)		(16 <sup>+</sup> ) $\rightarrow$ (15 <sup>+</sup> )
463.5	26.7(2.5)	0.66(0.08)	(15 <sup>+</sup> ) $\rightarrow$ (14 <sup>+</sup> )
478.1	2.7(0.5)		(11 <sup>+</sup> ) $\rightarrow$ (9 <sup>+</sup> )
495.8	15.6(3.3)	0.68(0.13)	(17 <sup>+</sup> ) $\rightarrow$ (16 <sup>+</sup> )
527.7	3.0(0.7)		(19 <sup>+</sup> ) $\rightarrow$ (18 <sup>+</sup> )
554.5	3.2(0.7)		(21 <sup>+</sup> ) $\rightarrow$ (20 <sup>+</sup> )
592.5	53.7(5.8)	1.36(0.19)	(12 <sup>+</sup> ) $\rightarrow$ (10 <sup>+</sup> )
650.5	10.6(1.6)	1.44(0.35)	(13 <sup>+</sup> ) $\rightarrow$ (11 <sup>+</sup> )
739.2	48.2(5.5)	1.33(0.21)	(14 <sup>+</sup> ) $\rightarrow$ (12 <sup>+</sup> )
807.0	12.6(1.6)	1.34(0.27)	(15 <sup>+</sup> ) $\rightarrow$ (13 <sup>+</sup> )
879.0	32.7(1.7)	1.43(0.25)	(16 <sup>+</sup> ) $\rightarrow$ (14 <sup>+</sup> )
910.8	13.0(2.9)	1.39(0.27)	(17 <sup>+</sup> ) $\rightarrow$ (15 <sup>+</sup> )
960.7	16.5(3.5)	1.45(0.28)	(18 <sup>+</sup> ) $\rightarrow$ (16 <sup>+</sup> )
993.0	4.7(1.0)	1.46(0.46)	(19 <sup>+</sup> ) $\rightarrow$ (17 <sup>+</sup> )
1045.5	14.1(2.6)	1.63(0.34)	(20 <sup>+</sup> ) $\rightarrow$ (18 <sup>+</sup> )
1072.2	5.7(1.3)	1.27(0.35)	(21 <sup>+</sup> ) $\rightarrow$ (19 <sup>+</sup> )
1135.2	2.6(0.8)		(22 <sup>+</sup> ) $\rightarrow$ (20 <sup>+</sup> )
1148.0	1.0(0.3)		(25 <sup>+</sup> ) $\rightarrow$ (23 <sup>+</sup> )
1148.3	1.4(0.4)		(23 <sup>+</sup> ) $\rightarrow$ (21 <sup>+</sup> )
1198.5	1.0(0.3)		(24 <sup>+</sup> ) $\rightarrow$ (22 <sup>+</sup> )
<b>Band 2</b>			
327.1	4.6(0.6)	0.64(0.19)	(13 <sup>+</sup> ) $\rightarrow$ (12 <sup>+</sup> )
344.4	6.4(1.0)	0.71(0.22)	(14 <sup>+</sup> ) $\rightarrow$ (13 <sup>+</sup> )
361.9	4.7(0.8)	0.59(0.17)	(12 <sup>+</sup> ) $\rightarrow$ (11 <sup>+</sup> )
426.5	11.7(1.5)	0.66(0.16)	(15 <sup>+</sup> ) $\rightarrow$ (14 <sup>+</sup> )
461.1	3.2(0.7)		(17 <sup>+</sup> ) $\rightarrow$ (16 <sup>+</sup> )
671.1	5.7(0.8)	1.35(0.48)	(14 <sup>+</sup> ) $\rightarrow$ (12 <sup>+</sup> )
689.3	11.6(1.0)	1.37(0.28)	(13 <sup>+</sup> ) $\rightarrow$ (11 <sup>+</sup> )
771.0	9.4(1.2)	1.36(0.34)	(15 <sup>+</sup> ) $\rightarrow$ (13 <sup>+</sup> )
901.5	3.6(0.7)	1.44(0.48)	(16 <sup>+</sup> ) $\rightarrow$ (14 <sup>+</sup> )
936.1	12.3(2.3)	1.41(0.27)	(17 <sup>+</sup> ) $\rightarrow$ (15 <sup>+</sup> )
1007.6	6.2(1.5)	1.48(0.45)	(19 <sup>+</sup> ) $\rightarrow$ (17 <sup>+</sup> )
1013.3	1.6(0.5)		(18 <sup>+</sup> ) $\rightarrow$ (16 <sup>+</sup> )
1046.5	0.7(0.2)		(20 <sup>+</sup> ) $\rightarrow$ (18 <sup>+</sup> )
1064.2	0.6(0.2)		(22 <sup>+</sup> ) $\rightarrow$ (20 <sup>+</sup> )
1066.0	4.2(1.2)	1.51(0.46)	(21 <sup>+</sup> ) $\rightarrow$ (19 <sup>+</sup> )
1106.8	1.7(0.4)		(23 <sup>+</sup> ) $\rightarrow$ (21 <sup>+</sup> )
<b>Linking transitions</b>			
95.5	5.0(1.0)	0.94(0.26)	(12 <sup>+</sup> ) $\rightarrow$ (11 <sup>+</sup> )
145.4	3.7(0.6)	0.85(0.25)	(14 <sup>+</sup> ) $\rightarrow$ (13 <sup>+</sup> )
253.0	12.5(1.1)	0.69(0.13)	(16 <sup>+</sup> ) $\rightarrow$ (15 <sup>+</sup> )
277.5	4.1(1.1)	0.66(0.19)	(18 <sup>+</sup> ) $\rightarrow$ (17 <sup>+</sup> )
315.5	2.2(0.5)		(20 <sup>+</sup> ) $\rightarrow$ (19 <sup>+</sup> )
496.5	27.9(3.2)	0.59(0.08)	(11 <sup>+</sup> ) $\rightarrow$ (10 <sup>+</sup> )
521.1	14.9(1.1)	0.72(0.08)	(12 <sup>+</sup> ) $\rightarrow$ (11 <sup>+</sup> )
542.5	25.1(2.5)	0.64(0.06)	(14 <sup>+</sup> ) $\rightarrow$ (13 <sup>+</sup> )
593.5	5.3(0.9)	0.74(0.2)	(13 <sup>+</sup> ) $\rightarrow$ (12 <sup>+</sup> )
637.0	8.4(2.5)	0.66(0.14)	(16 <sup>+</sup> ) $\rightarrow$ (15 <sup>+</sup> )
637.5	9.4(2.6)	1.38(0.31)	(11 <sup>+</sup> ) $\rightarrow$ (9 <sup>+</sup> )
679.8	2.1(0.6)		(16 <sup>+</sup> ) $\rightarrow$ (14 <sup>+</sup> )

TABLE I. (Continued.)

$E_\gamma$ (keV)	$I_\gamma$ (%)	ADO ratio	$I_i^\pi \rightarrow I_f^\pi$
739.0	6.4(1.5)	0.77(0.25)	(18 <sup>+</sup> ) $\rightarrow$ (17 <sup>+</sup> )
785.0			(22 <sup>+</sup> ) $\rightarrow$ (21 <sup>+</sup> )
791.8	3.8(1.0)	0.72(0.21)	(20 <sup>+</sup> ) $\rightarrow$ (19 <sup>+</sup> )
847.8	2.7(0.9)		(13 <sup>+</sup> ) $\rightarrow$ (11 <sup>+</sup> )
937.8	1.4(0.4)		(14 <sup>+</sup> ) $\rightarrow$ (12 <sup>+</sup> )
968.9	7.0(2.1)	1.34(0.37)	(15 <sup>+</sup> ) $\rightarrow$ (13 <sup>+</sup> )
1100.0	1.4(0.4)		(16 <sup>+</sup> ) $\rightarrow$ (14 <sup>+</sup> )

791.8, 847.8, 937.8, and 1100.0 keV between the two bands have been added to the level scheme. Sample spectra are shown in Fig. 2. The new observation of both  $M1$  and  $E2$  linking transitions between the two bands provides additional support to the judgment that the side band has the same parity as that of the yrast band. The alignment plots of band 1, band 2 and the known  $\pi h_{11/2} \otimes \nu g_{7/2}$  band, reported in Ref. [14], of  $^{126}\text{Cs}$  are shown in Fig. 3 where the  $\pi h_{11/2} \otimes \nu g_{7/2}$  band exhibits a sharp backbend at  $\hbar\omega = 0.41$  MeV caused by the rotational alignment of the first pair of  $h_{11/2}$  neutrons. The absence of a band crossing at this frequency for bands 1 and 2 in Fig. 3 indicates that the  $\nu h_{11/2}$  orbital is Pauli blocked in both bands, which suggests that an  $\nu h_{11/2}$  orbital is involved in the configurations of these bands. Moreover, the large initial alignments ( $\sim 6\hbar$ ) for both bands 1 and 2 strongly suggests that the  $h_{11/2}$  proton is involved in the configuration of bands 1 and 2.

All these experimental observations suggest that the side band has the same configuration  $\pi h_{11/2} \otimes \nu h_{11/2}$  as that of the yrast band. A possible interpretation of the side band is that it may result from the coupling between the unfavored signature of the  $\pi h_{11/2}$  orbital and the two signatures of the  $\nu h_{11/2}$  orbital. However, an energy splitting of  $\sim 200$  keV[see Fig. 4(a)] between the two bands is too small for the side band

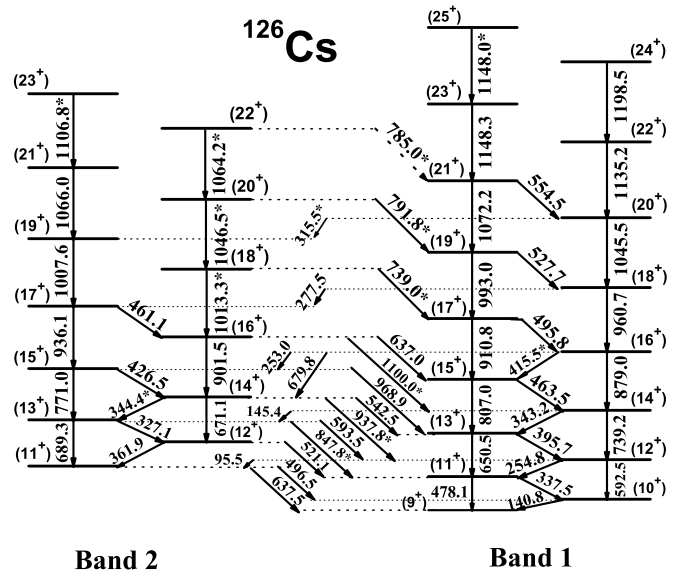


FIG. 1. Partial level scheme of  $^{126}\text{Cs}$ . New transitions observed in the present work are indicated with a star.

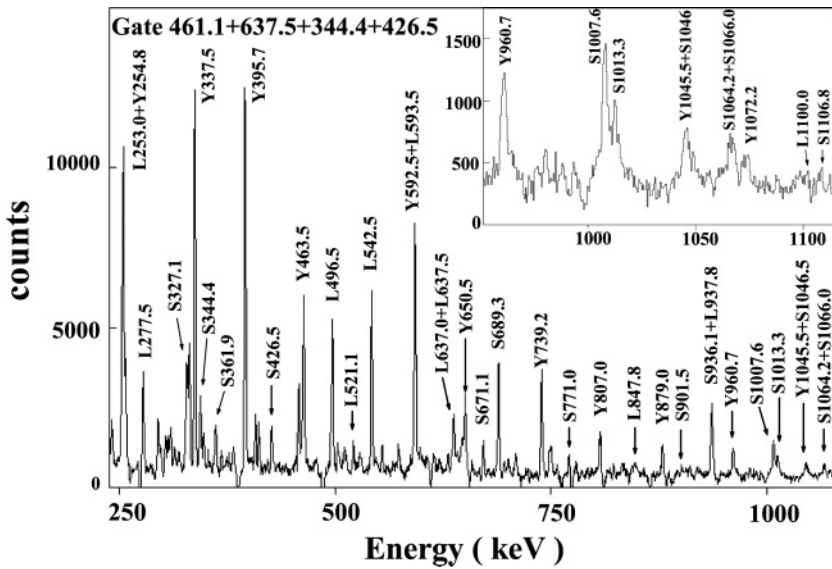


FIG. 2. Sample  $\gamma$ -ray coincidence spectra of the chiral doublet bands in  $^{126}\text{Cs}$ . Y, S, and L stands for transitions in the yrast band, the side band, and the linking transitions between the two bands, respectively.

to be interpreted as a band built on the unfavored signature of the proton orbital. An interpretation of  $\gamma$ -vibration coupled to the yrast band can also be ruled out because the  $\gamma$ -vibration energies are  $\geq 600$  keV in this mass region [3,6].

The observation of two near-degenerate  $\Delta I = 1$  bands has been considered as the fingerprint of the existence of chiral rotation. Recently, two further fingerprints, which must be observed in order to be consistent with the chiral geometry interpretation, were proposed by Koike *et al.* [16]. Firstly, the energy staggering parameter  $S(I) = [E(I) - E(I - 1)]/2I$  should possess a smooth dependence with spin since the particle and hole orbital angular momentum are both perpendicular to the core rotation in the chiral geometry. Secondly, due to the restoration of the chiral symmetry in the laboratory frame there are phase consequences for the chiral wavefunctions resulting in  $M1$  and  $E2$  selection rules which can manifest as  $B(M1)/B(E2)$  and  $B(M1)_{in}/B(M1)_{out}$  staggering as a function of spin and the odd spin members of the chiral bands have higher values relative to the even spin members for chiral

bands built on the configurations  $\pi h_{11/2} \otimes \nu h_{11/2}$  in nuclei with  $A \sim 130$ .

The degree of degeneracy of the two positive parity bands in  $^{126}\text{Cs}$  is indicated by the excitation energies of the band members as a function of spin as shown in Fig. 4(a). The two curves maintain a roughly constant energy difference of  $\sim 200$  keV showing near degeneracy within the observed spin interval. A plot of  $S(I)$  vs spin  $I$  is displayed in Fig. 4(b) where no significant spin dependence with spin is observed for  $I > 14\hbar$ . The reduced transition probability ratios  $B(M1)/B(E2)$  and  $B(M1)_{in}/B(M1)_{out}$ , which were deduced from the  $\gamma$ -intensities listed in Table I by using the relations (7) and (8) of Ref. [6], respectively, are shown in Fig. 5. The staggering of  $B(M1)/B(E2)$  and  $B(M1)_{in}/B(M1)_{out}$  ratios is evident both for the yrast and side band, and the odd-spin states have higher values than even-spin states except that the  $B(M1)/B(E2)$  staggering of the side band is less pronounced and it deviates from the staggering pattern at  $I = 14\hbar$ . The features of the two positive parity bands in  $^{126}\text{Cs}$ , displayed in

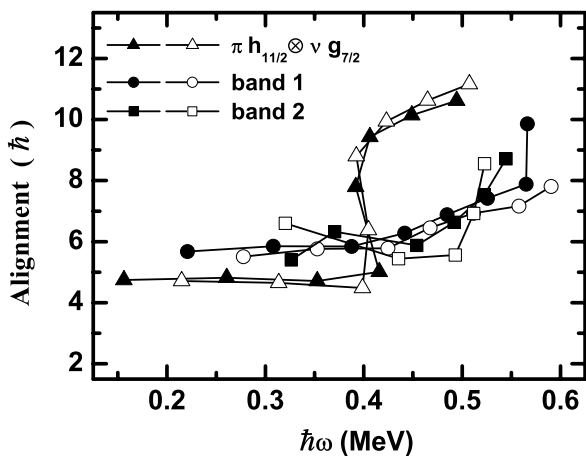


FIG. 3. Rotational alignments of bands in  $^{126}\text{Cs}$ . Harris parameters ( $J_0 = 17.0$ ,  $J_1 = 25.8$ ) [15] were used to subtract the angular momentum of the core.

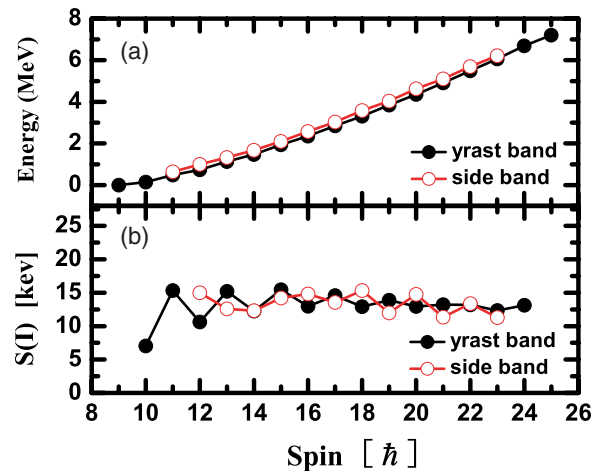


FIG. 4. (Color online) Excitation energy vs. spin (upper panel) and  $S(I)$  values vs. spin for the doublet bands in  $^{126}\text{Cs}$ .

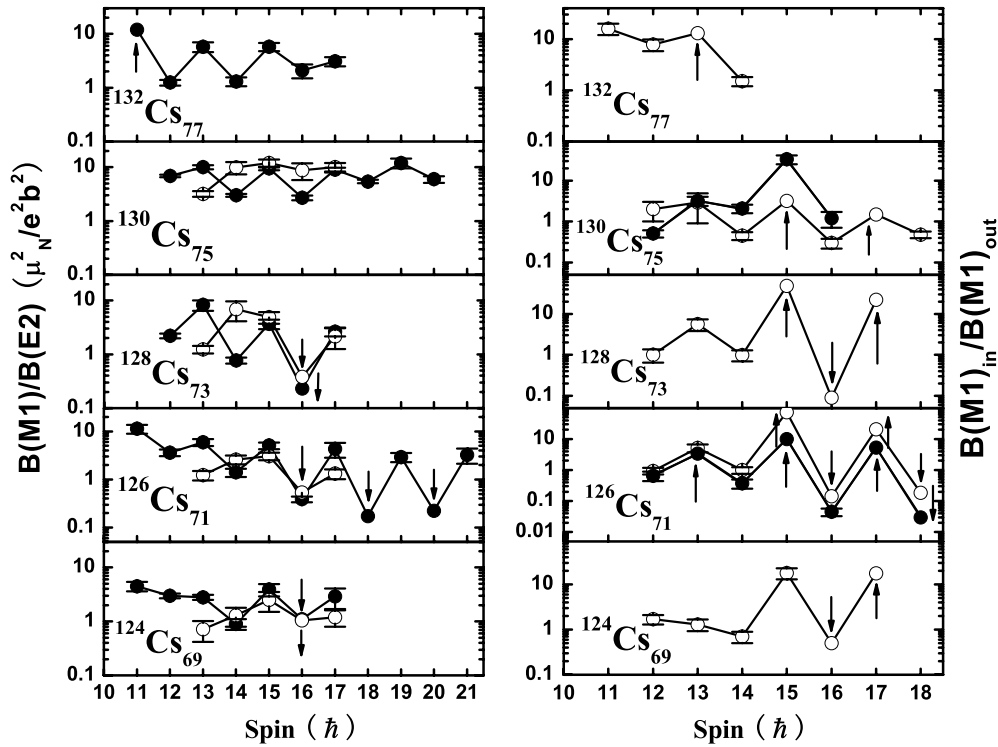


FIG. 5.  $B(M1)/B(E2)$  and  $B(M1)_{in}/B(M1)_{out}$  versus spin for yrast and side bands in  $^{126}\text{Cs}$  to compare with those in  $^{124}\text{Cs}$  [8],  $^{128}\text{Cs}$  [6],  $^{130}\text{Cs}$  [7],  $^{132}\text{Cs}$  [4]. Points with up (down) arrows represent lower (upper) limits.

Figs. 4 and 5, generally fit to the fingerprints of chiral rotation and therefore the two positive parity bands in  $^{126}\text{Cs}$  should be considered as candidate chiral doublet bands.

For comparison, the  $B(M1)/B(E2)$  and  $B(M1)_{in}/B(M1)_{out}$  ratios of the two positive parity bands in  $^{124}\text{Cs}$  [8],  $^{128}\text{Cs}$  [6],  $^{130}\text{Cs}$  [7], and  $^{132}\text{Cs}$  [4] are also displayed in Fig. 5. It is interesting to note that the similarities of the  $B(M1)/B(E2)$  and  $B(M1)_{in}/B(M1)_{out}$  ratios of these odd-odd Cs isotopes indicate that the chiral conditions do not change rapidly with neutron number  $N$  decreasing from  $N = 77$  ( $^{132}\text{Cs}$ ) to  $N = 69$  ( $^{124}\text{Cs}$ ). This is difficult to understand in view of the fact that the neutron Fermi level in  $^{124}\text{Cs}$  and  $^{126}\text{Cs}$  lies in or close to the middle of the  $\nu h_{11/2}$  subshell, where the orthogonal coupling between the proton and the neutron angular momentum, required by the chiral geometry, is not expected to occur.

In summary, high-spin states in odd-odd  $^{126}\text{Cs}$  have been studied by using the  $^{116}\text{Cd}(^{14}\text{N}, 4n)^{126}\text{Cs}$  reaction. The

previously reported two positive-parity bands have been confirmed and extended and new linking transitions between the two bands have been observed. The properties of the two positive-parity bands show general agreement with the fingerprints of chiral rotation and thus these two bands are suggested to be the candidate chiral doublet bands in  $^{126}\text{Cs}$ . The  $B(M1)/B(E2)$  and  $B(M1)_{in}/B(M1)_{out}$  ratios deduced from the present work show similar staggering pattern as those in  $^{124,128,130,132}\text{Cs}$ . The observation of chiral doublet bands in  $^{126}\text{Cs}$  indicates that the chiral conditions do not change rapidly with decreasing neutron number in these odd-odd Cs isotopes.

This study was supported by the National Natural Science Foundation (Grant Nos. 10275028, 10205006 and 10105003), Research Fund for the doctoral Program of Higher Education (No. 20030183055) and the Major State Research Development Programme (No. G2000077405) of China.

- [1] S. Frauendorf and J. Meng, Nucl. Phys. **A617**, 131 (1997).  
 [2] T. Koike, K. Starosta, C. J. Chiara, D. B. Fossan, and D. R. LaFosse, Phys. Rev. C **63**, 061304(R) (2001).  
 [3] K. Starosta *et al.*, Phys. Rev. Lett. **86**, 971 (2001).  
 [4] G. Rainovski *et al.*, Phys. Rev. C **68**, 024318 (2003).  
 [5] R. A. Bark, A. M. Baxter, A. P. Byrne, G. D. Dracoulis, T. Kibedi, T. R. McGoram, and S. M. Mullins, Nucl. Phys. **A691**, 577 (2001).  
 [6] T. Koike, K. Starosta, C. J. Chiara, D. B. Fossan, and D. R. LaFosse, Phys. Rev. C **67**, 044319 (2003).  
 [7] A. J. Simons *et al.*, J. Phys. G **31**, 541 (2005).  
 [8] A. Gizon *et al.*, Nucl. Phys. **A694**, 63 (2001).  
 [9] X. Li *et al.*, Chin. Phys. Lett. **19**, 1779 (2002).  
 [10] T. Komatsubara *et al.*, Nucl. Phys. **A557**, 419c (1993).  
 [11] M. Piiparinen *et al.*, Nucl. Phys. **A605**, 191 (1996).  
 [12] S. Wang *et al.*, J. Phys. G **32**, 283 (2006).  
 [13] Y. Liu, J. Lu, Y. Ma, S. Zhou, and H. Zheng, Phys. Rev. C **58**, 1849 (1998).  
 [14] X. Li *et al.*, Eur. Phys. J. A **17**, 523 (2003).  
 [15] Y. Liang *et al.*, Phys. Rev. C **42**, 890 (1990).  
 [16] T. Koike *et al.*, FNS2002, Berkeley, CA, 2002, AIP Conf. Proc. No. 656, edited by P. Fallon and R. Clark (AIP, Melville, New York, 2003), p. 160.